fluids

MDPI

Article

Rheological Features of Aqueous Polymer Solutions Tailored by Hydrodynamic Cavitation

Santiago Nicolás Fleite [1,2,3], María del Pilar Balbi [1,2], María Alejandra Ayude [4,5] and Miryan Cassanello [1,2,*]

[1] Instituto de Tecnología de Alimentos y Procesos Químicos (ITAPROQ), CONICET, Universidad de Buenos Aires, Buenos Aires C1428BGA, Argentina; fleite@di.fcen.uba.ar or fleite@agro.uba.ar (S.N.F.); mpbalbi@fi.uba.ar (M.d.P.B.)
[2] Laboratorio de Reactores y Sistemas para la Industria (LARSI), Departamento de Industrias, FCEyN, Universidad de Buenos Aires, Buenos Aires C1428BGA, Argentina
[3] Cátedra de Química Inorgánica y Analítica, Facultad de Agronomía, Universidad de Buenos Aires, Buenos Aires C1120AAQ, Argentina
[4] Departamento de Ingeniería Química y de Alimentos, Universidad Nacional de Mar del Plata (UNMdP), Mar del Plata B7600FDQ, Argentina; mayude@fi.mdp.edu.ar
[5] División Catalizadores y Superficies, Instituto de Investigaciones en Ciencia y Tecnología de Materiales (INTEMA), CONICET, Universidad Nacional de Mar del Plata (UNMdP), Mar del Plata B7600FDQ, Argentina
* Correspondence: miryan@di.fcen.uba.ar; Tel.: +54-11-52859029

Abstract

Hydrodynamic cavitation (HC) has emerged as a versatile method for modifying the rheological properties of polymer solutions, offering advantages such as scalability and operational simplicity. This work investigates the effect of HC on aqueous polyacrylamide (PAM) solutions, focusing on viscosity and viscoelasticity changes as a function of the number of passes through a vortex-type HC device and the presence of dissolved salts ($CaCl_2$ or KCl). Viscosity measurements were modeled using the power law equation, while oscillatory tests were used to determine storage and loss moduli. The results show that HC substantially reduced viscosity and elastic behavior, with the degree of modification strongly influenced by the number of passes. A critical molecular size limit was suggested, below which further degradation becomes limited. Salt addition enhanced depolymerization, likely due to charge screening, hydrodynamic radius reduction, and the increased solubility and mobility of polymer chains within cavitation bubbles. HC eliminated elasticity in all cases, yielding solutions with near-Newtonian behavior. The transformation is attributed to molecular weight reduction and changes in molecular size distribution. These findings support the use of HC as a practical approach to tailor the flow properties of PAM solutions, while highlighting intrinsic limitations imposed by cavitation dynamics and polymer chain dimensions.

Keywords: hydrodynamic cavitation; polyacrylamide aqueous solution; viscosity; rheological behavior

check for updates

Academic Editor: Rui Han

Received: 31 May 2025
Revised: 24 June 2025
Accepted: 27 June 2025
Published: 29 June 2025

Citation: Fleite, S.N.; Balbi, M.d.P.; Ayude, M.A.; Cassanello, M. Rheological Features of Aqueous Polymer Solutions Tailored by Hydrodynamic Cavitation. *Fluids* **2025**, *10*, 169. https://doi.org/10.3390/fluids10070169

Copyright: © 2025 by the authors. Licensee MDPI, Basel, Switzerland. This article is an open access article distributed under the terms and conditions of the Creative Commons Attribution (CC BY) license (https://creativecommons.org/licenses/by/4.0/).

1. Introduction

Water-soluble, biodegradable, and biocompatible polymers are widely used for diverse industrial applications. They are typically employed as stabilizers and thickeners for medicines, cosmetics, and coatings, for assisting petroleum extraction, and for wastewater remediation. Although available with different grades, their high molecular weight and broad molar mass distribution can pose handling and performance challenges. Hence,

different methods have been proposed and studied to partially reduce the polymer chains after their synthesis, to fit desired conditions [1]. Moreover, the increasing use of these polymers has led to large amounts of polymer-bearing wastewater, which is difficult to process due to its high viscosity. This highlights the need for viscosity reduction, typically achieved through depolymerization by thermal, chemical, mechanical, and enzymatic or biological methods [2,3].

Among the mechanical methods used to post-process or treat polymer aqueous solutions, hydrodynamic cavitation appeared as a promising alternative due to its simple application and ease of scalability [4,5]. Cavitation involves the formation of small bubbles, called cavities, which initially grow and then are compressed and finally collapse, inducing local extreme conditions [6–8]. Apart from high local temperatures, the released energy can result in mechanical effects related to shock waves, microjets, and high shear stress. In addition, the implosion generates highly reactive species, like hydroxyl radicals, which can act at the molecular level to modify polymer chain length. Yan et al. [9] evidenced that mechanical forces like those exerted by cavitation generally lead to cleavage of polymer chains around the center, generating molecules of significantly lower molar mass with a narrow distribution. On the other hand, highly active species, which can also be formed by cavitation, cleave the polymer chains randomly, also leading to smaller molecules but with a broader molar mass distribution.

Examples of polymer aqueous solutions that have been modified through cavitation are carboxymethyl cellulose (CMC) and hydroxypropyl methyl cellulose (HPMC). It was shown that the use of acoustic or hydrodynamic cavitation can successfully cleave the cellulose glycosidic bonds of CMC and HPMC [1,10]. CMC is extensively used for diverse applications in the food and cosmetic industries. HPMC is a non-ionic, semi-synthetic derivative of cellulose commonly applied in medicine for controlled drug delivery and in the food industry as a stabilizer. Another polymer that has been subjected to ultrasonic (US) cavitation for tuning the aqueous solution features is Konjac glucomannan (KGM) [11]. KGM is a polysaccharide used for pharmaceutical and biotechnological applications. However, modifications of the naturally extracted polymer are required to meet the necessary conditions (solubility, viscosity, etc.). US cavitation was found to be appropriate for reducing the molecular weight and viscosity without occasioning changes in the chemical nature of this polymer [11]. The authors found that the initially shear-thinning behavior of a 0.25% (w/v) KGM aqueous solution became Newtonian by applying US cavitation for more than 4 min.

Polyacrylamide (PAM) is also a polymer that has been extensively used in the industry, along with its derivatives. Its main applications are found in water treatment, the textile industry, and especially in oil recovery [12–14]. Aqueous PAM solutions are frequently employed to enhance the sweep capability of injection fluids in oil recovery, as their high viscosity improves oil displacement. However, the synthesis of PAM often results in molar masses and distributions that do not fully meet the application requirements. Hence, post-processing of commercial PAM is used to tailor the molecular weight by partially cleaving the polymer chains.

Thermal, chemical, and enzymatic methods have been proposed to modify the molar mass and distribution of PAM [3], but these treatments are frequently complex and expensive. In contrast, cavitation, either ultrasonic or hydrodynamic, and its combination with other advanced oxidation processes, provides a simple, cleaner, and faster route to reduce the molar mass of PAM chains to desirable levels. Prajapat and Gogate [13] demonstrated that the conditions of hydrodynamic cavitation (HC), applied using a slit venturi device, significantly influence the viscosity reduction in the polymer solution. These authors also combined HC with other advanced oxidation processes to further enhance polymer degra-

dation. HC offers strong potential for scale-up with relatively low investment and operating costs [15,16]. It arises from a perturbation in the flowing fluid that moves the pressure below the solvent (water) vapor pressure, thus inducing the formation of vapor cavities. As the fluid continues downstream, pressure increases and bubbles are compressed and finally collapse violently, producing effects comparable to those of the ultrasound cavitation.

Recently, Zhang et al. [14] used simulations to analyze the impact of bubble collapse on PAM degradation efficiency. They concluded that the local shear after collapse induces stretching of C–C bonds and expansion of C–C–C bond angles in the PAM main chain, leading to fragmentation of the molecules. This mechanical degradation proceeds without significant change in the chemical structure, and the bond breaking occurs in the central region of the collapsing bubble.

In this context, the aim of the present work is to examine the suitability of HC as a method for tailoring the rheological properties of polymeric solutions. PAM is used as a model polymer due to its widespread application in oil recovery. Aqueous PAM solutions at different concentrations are subjected to HC using a vortex-type cavitation device, which achieves cavitation inception at lower pressure drops [17,18]. This study focuses particularly on the effects of the number of passes through the cavitation device and the presence of dissolved salts in the solution.

2. Materials and Methods

2.1. Experimental Setup

The setup for subjecting the polymer solutions to hydrodynamic cavitation (HC) is schematized in Figure 1. The cavitation device was a vortex diode type with a throat diameter of 6 mm, procured from VIVIRA Process Technology Pvt. Ltd. (100 NCL Innovation Park, Dr Homi Bhabha Rd, Pune, Maharashtra 411008, India). A batch assembly powered by a 1 HP centrifugal pump was used. It contained regulating valves to control the flow rate and a cryostat to keep the temperature at 20 ± 1 °C.

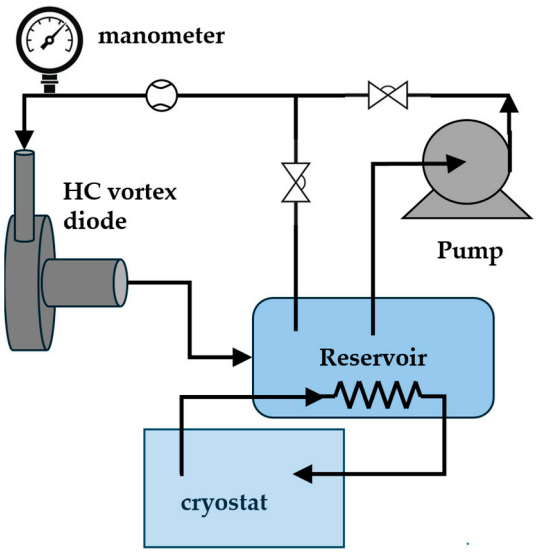


Figure 1. Experimental setup.

The pressure drop through the cavitation device was varied between 2 and 3.5 bar, resulting in liquid flow rates in the range of 3 to 6 L/min. Experiments were carried out for different number of passes through the HC device to analyze the effect on the rheological characteristics of the aqueous polymer solutions. The number of passes (n_p) roughly gives how many times the whole liquid passes through the cavitation device [16]. The time (t) needed for a given number of passes (n_p) depends on the liquid flow rate through the

cavitation device (Q) and the volume of the liquid in the reservoir tank (V), as expressed in Equation (1).

$$t = n_p\ V/Q \quad (1)$$

The vortex-type cavitation device consists in a bidirectional fluid flow system, in which the inlet flow enters a swirl chamber where high-speed rotation is achieved. The fluid exits only through a centered outlet channel perpendicular to the base of the swirl chamber, with a narrowing point called the throat [17,18]. The high-speed rotation induces the formation of cavitation bubbles due to the sharp decrease in the liquid pressure close to the device throat. Further details of the vortex cavitation device can be found in studies devoted to the analysis of the features of this system [17–21].

Cavitation inception in vortex-type cavitation is achieved at lower pressure drops than those required in Venturi or orifice plate configurations [18]. The cavitation bubbles or cavities formed in the throat region are sharply compressed when the liquid pressure is recovered far from the throat, leading to bubble collapse. During this period, extreme temperatures and pressures are locally reached. By single bubble dynamics simulation, Pandit et al. [22] have estimated peak temperatures over 5000 K and local pressures of around 1000 Pa for this device geometry, likely leading to the formation of supercritical water (SCW) domains prior the collapse. Simulations indicated that bubble diameters may reach ~20 μm, which are reduced to around 3 μm before collapsing.

In this work, cavitation inception was verified at pressure drop ~0.9 bar for the 1 g/L PAM solution using acoustic and vibration sensors, following Ranade et al. [20]. A change from around 12 to 60 dB was found at inception, consistent with data reported in [20]. It is worthwhile mentioning that Thacker et al. [23] have studied the influence of liquid viscosity on the pressure drop required for cavitation inception in this system, using glycerol aqueous solutions. The pressure drop range studied in this work is above the pressure drop required for cavitation inception in a similar system for solutions with viscosities of 61 mPa s. The PAM solutions used in this work have significantly lower viscosities. Therefore, under the experimental conditions examined, hydrodynamic cavitation was certainly achieved.

2.2. Materials

High-molar mass cationic polyacrylamide (PAM) FZ-81 from Faisan S.A., León XIII Nº 154, CP 1888 Florencio Varela, Argentina, was used for preparing the polymer solutions. The skeletal structure of the PAM used is shown in Figure 2. As additives, analytical-grade potassium chloride (KCl) and calcium chloride ($CaCl_2$) were used in 0.01 M concentrations. All solutions were prepared with distilled water.

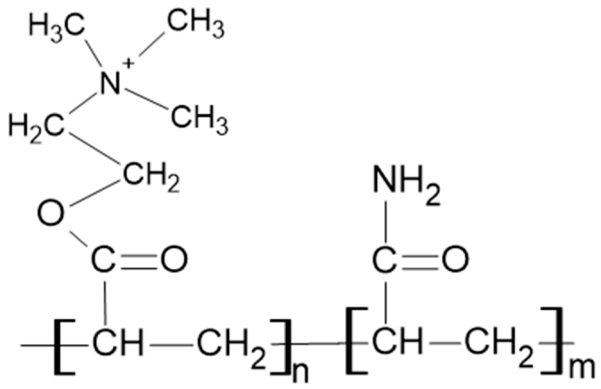


Figure 2. Skeletal structure of the cationic polyacrylamide used.

2.3. Viscosity and Viscoelasticity Measurement

Shear stress versus shear rate curves were measured using a plate-cone (CPE-40) Brookfield LVDV-II+ programmable viscometer and WINGATHER® and DVLoader® programs (AMETEK Brookfield, 11 Commerce Boulevard, Middleboro MA 02346, USA). The influence of PAM concentration on the polymer aqueous solution viscosity was first assessed, as well as the effect of adding 0.01 M of KCl or $CaCl_2$. Then, the solutions were subjected to HC for a given number of passes to analyze the influence on the rheological properties. Viscosity measurements were performed under a controlled temperature of 20 ± 0.1 °C. The rheological curves were analyzed using the Ostwald–de Waele model (i.e., the power law model), as expressed in Equation (2) [24]:

$$\tau = k\,\gamma^{n} \quad (2)$$

where τ is the shear stress (Pa), γ is the shear rate (Hz), k is the consistency index (Pa·s^n), and n is the flow behavior index (dimensionless).

Viscoelastic properties were assessed for the solutions before HC treatment and after 500 passes, using a Modular Compact Rheometer (Model MCR 102e, Anton Paar, Graz, Austria) controlled by RheoCompass software (21 CFR Part 11, 1.21.805 version, Anton Paar). Linear viscoelastic properties were determined through small-amplitude oscillatory shear (SAOS) tests [12,25,26]. A strain sweep was imposed at a fixed angular frequency to determine the linear viscoelastic range (LVR). The applied strain of shear amplitude (γ_0) and angular frequency (ω) varies with time (t) according to Equation (3).

$$\gamma = \gamma_0 \sin(\omega t) \quad (3)$$

Within the LVR, the resulting shear stress (τ) changes with the same frequency but may be shifted in phase. The oscillating shear stress function can be expressed in terms of the sine and cosine of the angular velocity, as expressed in Equation (4), where G′ is called the storage modulus and G″ is the loss modulus. G′ and G″ can also be a function of the angular frequency.

$$\tau = \gamma_0 \left(G' \sin(\omega t) + G'' \cos(\omega t)\right) \quad (4)$$

G′ and G″ were determined from the SAOS test with a strain sweep (0.1–100%) at a fixed frequency of 2 Hz. Briefly, the G′ modulus is related to the solid-like elastic behavior, the trend to return to the initial configuration after the deformation, while the G″ modulus is related to the viscous component. Thus, if G′ > G″, the sample behaves more like a rigid solid experiencing reversible deformation (elasticity). If G′ < G″, the sample behaves like a fluid, experiencing irreversible deformation. A useful magnitude to summarize the analysis is the ratio G″/G′, also referred to as tan(δ), where δ is the phase shift. If this ratio is < 1, the sample tends to behave as an elastic solid in the LVR. If >1, the sample behaves more like a fluid [25,26].

3. Results and Discussion

3.1. Polymer Solution Viscosity

The PAM solutions' rheological curves can be well represented by Equation (2) with increasing deviations from Newtonian behavior as the PAM concentration increases. Thus, the consistency index increases while the index of flow behavior becomes progressively lower than 1 for higher polymer concentrations (Table 1 and Figure 3a).

Table 1. Effect of PAM concentration and addition of salts on indexes of Equation (2) used to describe the rheological behavior of the aqueous solutions.

PAM Concentration	Salt Concentration	Consistency Index, k (Pa·s^n)	Index of Flow Behavior, n (Dimensionless)
0.02 g/L	–	0.003 ± 0.0002	0.91 ± 0.05
0.10 g/L	–	0.009 ± 0.0005	0.76 ± 0.04
0.50 g/L	–	0.025 ± 0.002	0.67 ± 0.03
0.80 g/L	–	0.064 ± 0.003	0.57 ± 0.03
1.10 g/L	–	0.119 ± 0.008	0.53 ± 0.03
1.30 g/L	–	0.299 ± 0.015	0.40 ± 0.02
1.00 g/L	–	0.092 ± 0.007	0.55 ± 0.03
1.00 g/L	0.01 M KCl	0.043 ± 0.003	0.65 ± 0.03
1.00 g/L	0.01 M $CaCl_2$	0.026 ± 0.002	0.70 ± 0.04

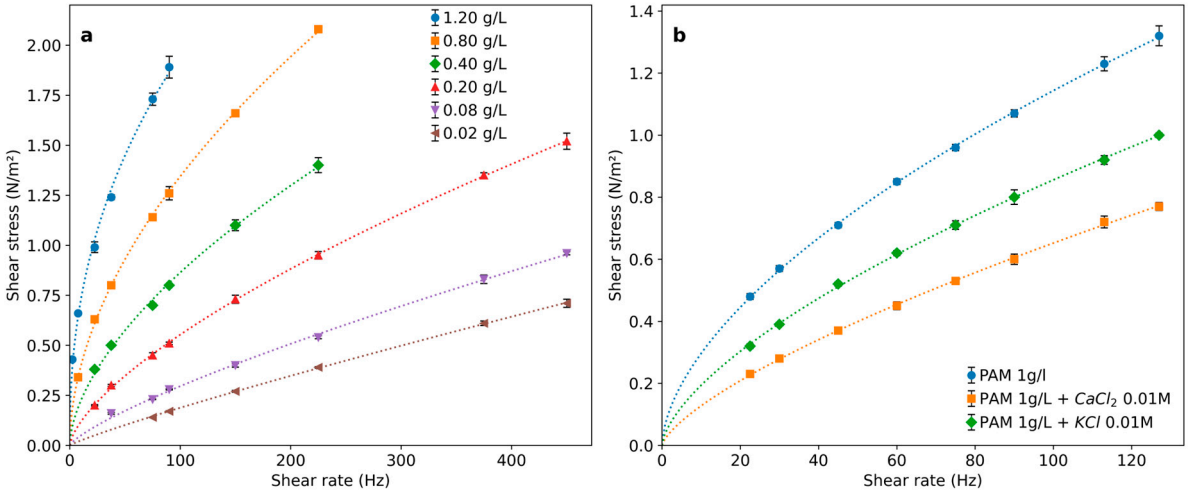


Figure 3. Rheological behavior of PAM solutions for (**a**) different concentrations and (**b**) with addition of salts with different ionic forces.

Salt addition induces a significant modification of the flow behavior (Table 1 and Figure 3b), which depends on the cation charge. The solution viscosity decreases, and the flow index becomes closer to those of Newtonian solutions. This effect is coincident with the one reported for PAM solutions containing high salt concentrations characteristic of oil-well wastewaters [12,27].

Polymers are generally present as individual chains in dilute and semidilute solutions. Their conformations can vary from highly extended to tightly coiled, depending on the interactions among chains (attractive or repulsive) and between the polymer and the solvent. PAM is generally in the form of extended linear chains in semidilute aqueous solutions. The addition of an inert salt, like NaCl or $CaCl_2$, negatively affects the interactions among the polymer chains, reducing the repulsion due to electrostatic screening. For this reason, the addition of an inert salt induces a decrease in PAM solutions' viscosity [12]. Recently, Arok et al. [26] have evidenced that PAM aqueous solutions above a certain concentration tend to form gel-like structures, as evidenced from the viscoelastic characteristic of the solutions (elastic modulus larger than viscous modulus) and from light scattering and electrophoretic experiments. When NaCl was added to the solutions above a certain concentration, electrostatic forces induce the disappearance of the gel-like structure, simultaneously decreasing the solution viscosity.

3.2. Effect of the Number of Passes and the HC Pressure Drop on Polymer Rheology

Figure 4 illustrates the effect of treating a 1 g/L PAM solution with HC during a different number of passes through the vortex-type HC device. Different flow rates through the vortex diode lead to different pressure drops between 2 and 3.5 bars being imposed.

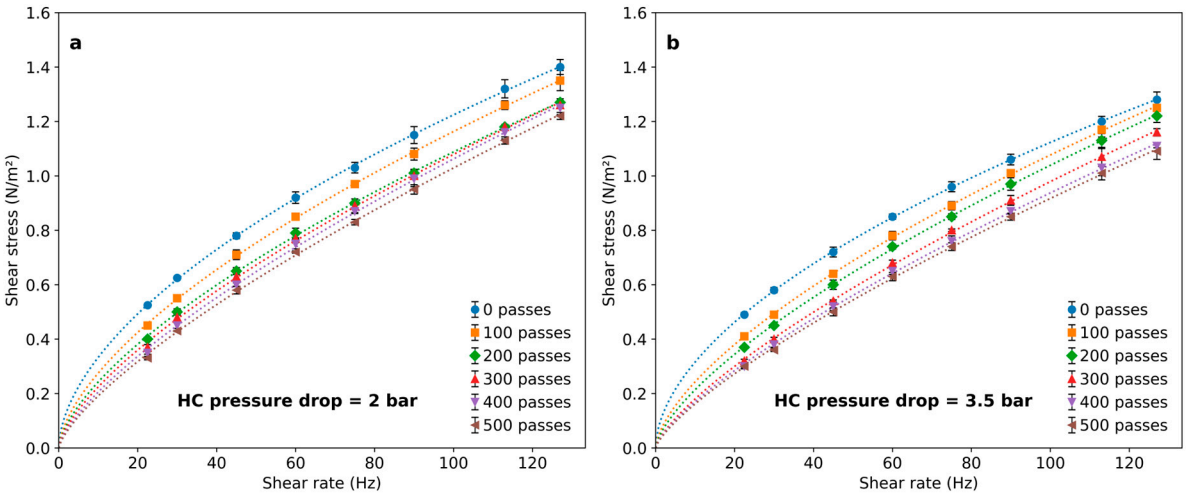


Figure 4. Rheological behavior of PAM solutions after a different number of passes through the cavitation device for (**a**) 2 bar pressure drop and (**b**) 3.5 bar pressure drop.

In all cases, polymer solutions exhibited a decrease in viscosity following HC treatment. This effect was dependent on the number of passes and only slightly associated with the pressure drop in the HC device. The effect was notable after 100 passes and became progressively less important for an increasing number of passes, leading to marginal differences above 400 passes. The flow indexes calculated by fitting results to Equation (2) are shown in Figure 5. The results indicate that the polymer viscosity can be reduced by imposing HC with a vortex diode device, and the number of passes is a significant variable to set for achieving rheological modifications.

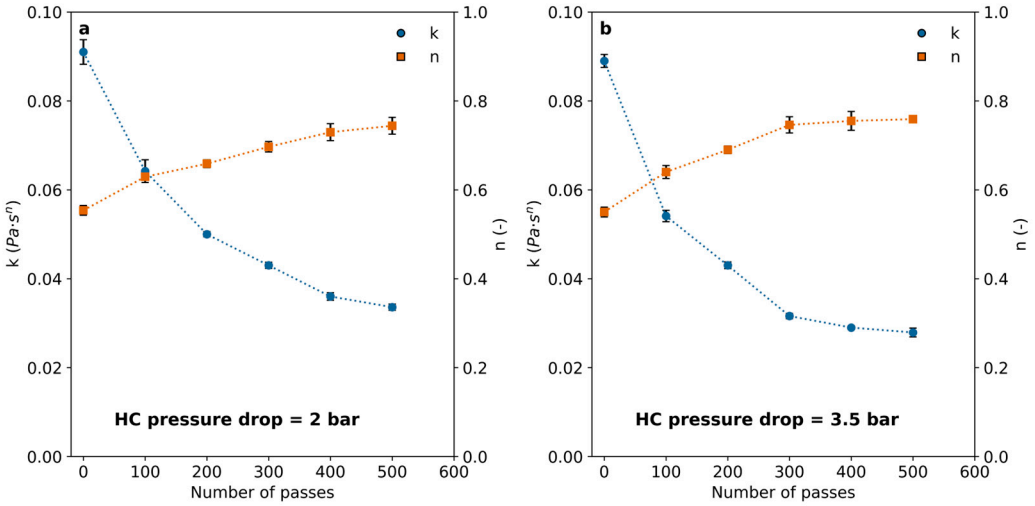


Figure 5. Consistency (k) and flow behavior (n) indexes (Equation (2)) calculated for the PAM solutions after a different number of passes through the cavitation device for (**a**) 2 bar pressure drop and (**b**) 3.5 bar pressure drop through the vortex diode.

The consistency index (k) decreased significantly in all cases, while the index of flow behavior slowly increased, reaching a plateau close to 0.8 for all the examined pressure drops within the range between 2.0 bar and 3.5 bar, remaining almost unchanged for more

than 400 passes. The effect of pressure drop through the HC device did not appear to have a significant impact when considering the measurement uncertainties, suggesting a mechanism distinct from those typically involved in HC-enhanced chemical reactions.

Previous studies [28] identified an optimal pressure drop of 2.8 bar for vortex-type hydrodynamic cavitation (HC) devices used in the degradation of organic compounds. A strong dependence on head loss (or pressure drop) is commonly reported in the literature, as it is associated with cavitation collapse intensity, radical formation, pyrolysis, and the generation of supercritical water (SCW) [15,22,28,29]. Polymer molecules are prone to cleavage by the exerted mechanical forces during the collapse or through chemical degradation by pyrolysis, radical attack, and other reactions, such as those observed in SCW reactors [30]. The interaction between bubble size and polymer chain size may influence the predominant mechanism. Mechanical forces can selectively affect molecules above a certain size threshold, which cannot be entrapped within the bubbles. In contrast, chemical mechanisms would be responsible for the degradation of short-chain molecules. Pandit et al. [22] have estimated cavitation bubbles with sizes in the order of a few microns before collapsing for this system. In addition, the extreme conditions that can be attained suggest that SCW domains are likely to appear. These domains within the cavities may contribute to capturing polymer chains that are below a critical length and subject them to chemical degradation. Intermediate length chains, too large to get entrapped in the bubbles but too small to be affected by mechanical forces, may remain stable in the liquid bulk. This phenomenon is sketched in Figure 6. Large polymer chains, which are unlikely to enter cavitation bubbles, experience intense localized mechanical stress that leads to chain cleavage, as predicted by Zhang et al. [14]. Additionally, the formation of SCW may further promote depolymerization through the oxidation of smaller chains [30]. Previous works that used acoustic or hydrodynamic cavitation to treat polymer aqueous solutions have evidenced molecular size reduction by size-exclusion chromatography [1,9]. The trend towards molar weight reduction was evidenced in these works. In addition, Yan et al. [9] found that the molar mass distributions of chitosan became narrower for increasing HC time (i.e., larger number of passes), starting from a mean of circa 10^6 Da and concentrating progressively in the range of 0–50,000 Da, suggesting that there is a molecular size limit below which there is a minimal effect of HC. These authors showed that after 30 min HC, they obtained a broad molar mass distribution, reaching values up to ~2×10^6 Da, with a mean of around 10^6 Da. In contrast, for 120 min HC, the distribution reduced to a range up to ~2.5×10^5 Da, with a mean of ~50,000 Da and a mode one order of magnitude larger.

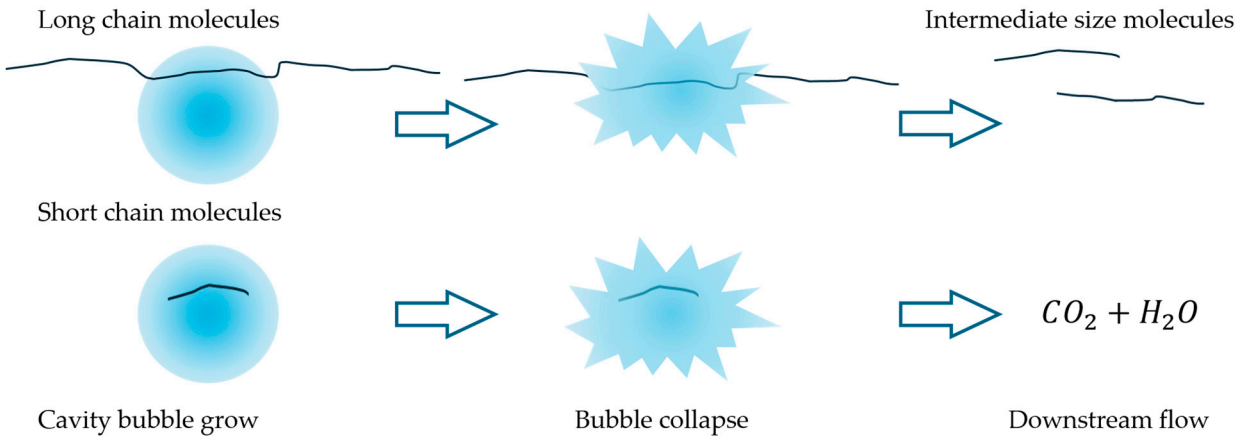


Figure 6. Sketch of the idealized polymer molecules' evolution under HC. Long-chain molecules can be cleaved to relatively stable intermediate-size molecules by mechanical shear or by partially entering the bubble. Short-chain molecules can enter the bubbles and be further oxidized. As a result, polymer molecules of intermediate size are formed, and further depolymerization by HC cannot be achieved.

Hence, while relatively small and large chains are degraded by pyrolysis or cleaved by shear forces, respectively, there may exist an intermediate size range that is too large to enter the bubble and undergo pyrolysis, yet too small to experience sufficient mechanical shear. For this reason, after a certain number of passes, the effect of HC becomes negligible—even if the solution's viscosity remains well above that of water. Therefore, HC can reduce polymer molecular size only up to a certain limit. However, this limit could potentially be shifted by redesigning the HC device to generate mechanical stresses at a different characteristic length scale, consistent with the Kolmogorov scale of turbulence energy dissipation.

3.3. Effect of the Number of Passes and the Salt Concentration on Polymer Rheology

The effect of having salts dissolved in the 1 g/L PAM solutions on the rheological modifications occasioned by a different number of passes through the HC device are illustrated in Figure 7. The initial solution viscosity was already reduced when salt was added, particularly for the higher-charged cations (Figure 3b). After subjecting them to HC, a marked reduction in the solution viscosity was observed. Apparently, the presence of charged ions in the solution enhances the effect of HC, which is particularly high during the first 100 passes. The flow behavior index tends to be one after 500 passes, indicating that the solutions approach Newtonian behavior. This is particularly evident for the PAM solution containing $CaCl_2$ (Figure 7b).

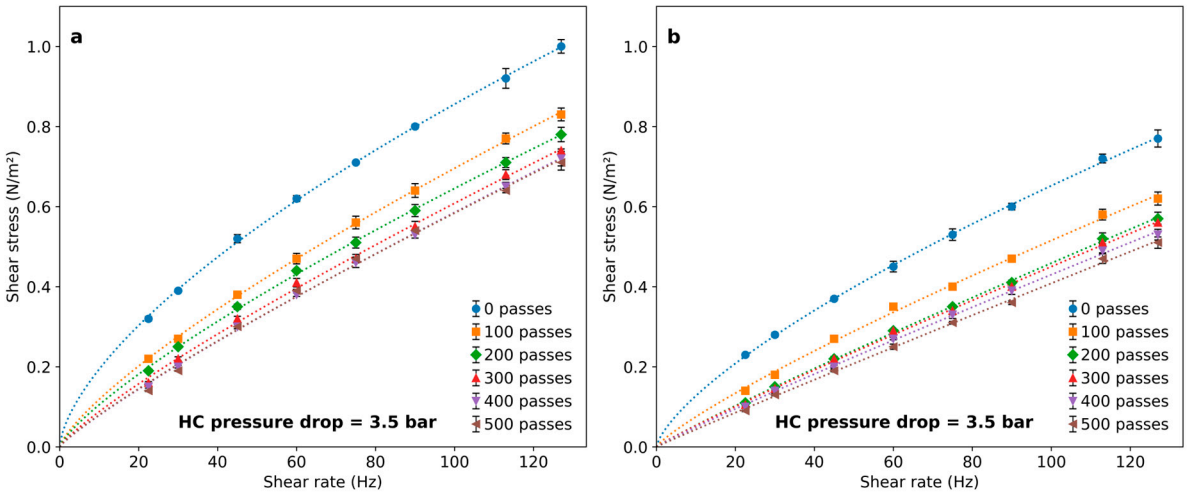


Figure 7. Rheological behavior of PAM solutions with salt addition, after a different number of passes through the cavitation device. Final salt concentration: (**a**) 0.01 M KCl; (**b**) 0.01 M $CaCl_2$.

The addition of salt significantly decreased the apparent viscosity, as it alters the structure and distribution of PAM chains. According to Arok et al. [26], the ions in the solution promote a charge-screening effect, weakening intermolecular interactions and inducing a transition from a gel-like macromolecular network to smaller, cluster-like structures. Regarding HC, salt addition accelerated the depolymerization rate of PAM in all cases and extended the effectiveness of HC over a greater number of passes, as the solutions continued to approach the viscosity of water. It has been proposed that salt addition induces a salting-out effect, enhancing the solubility of polymer short chains within the SCW domain inside the cavity bubbles while they grow [7]. Thus, increased PAM solubility in SCW, combined with enhanced chain mobility, likely increased the probability of partial or complete chain incorporation into cavitation bubbles, as sketched in Figure 8. Another factor to consider is the decrease in PAM hydrodynamic radius observed with the addition of bivalent ions (Ca^{2+} and Mg^{2+}) [31,32]. This would enhance the PAM chains' mobility and facilitate their entry, partially or entirely, into cavitation bubbles.

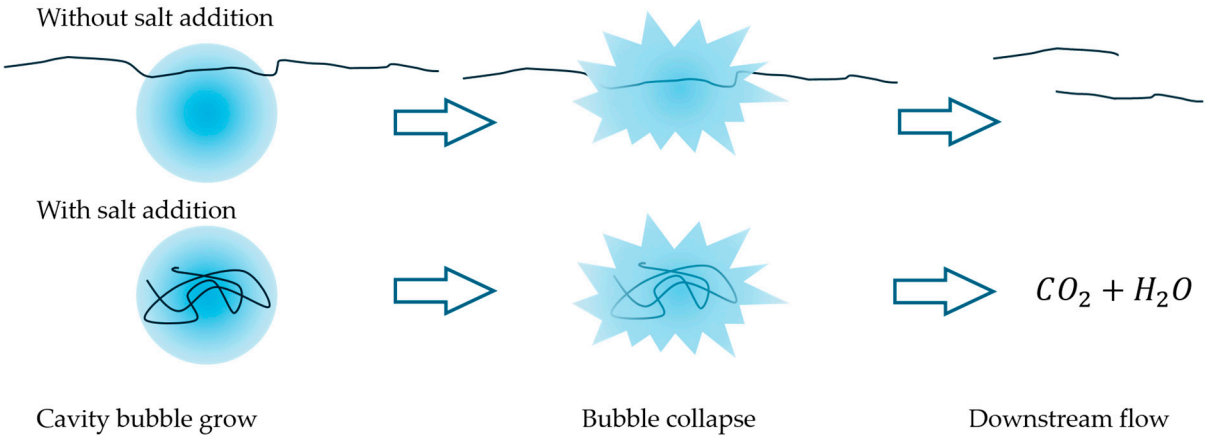


Figure 8. Sketch of the salt effect on HC performance. The addition of salt reduces the hydrodynamic radius of polymer chains, allowing larger molecules to enter cavitation bubbles and undergo degradation. As a result, the critical size limit decreases, enabling further depolymerization and leading to lower final viscosities.

The flow behavior index (n), which tends toward more Newtonian-like values with an increasing number of passes and with salt addition (Figure 9), suggests a reduction in both the average molecular weight and the strength of water–polymer interactions. This effect was clearly more pronounced in salt-containing solutions, with the $CaCl_2$-PAM solution nearly reaching ideal Newtonian behavior after 500 passes (Figure 9b).

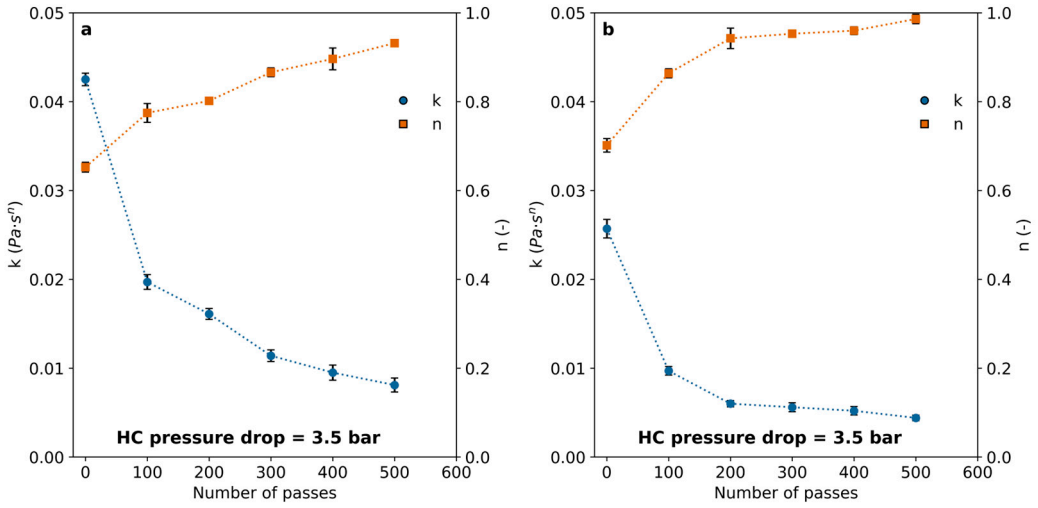


Figure 9. Consistency (k) and flow behavior (n) indexes (Equation (2)) calculated after a different number of passes through the cavitation device for PAM solutions with (**a**) 0.01 M KCl or (**b**) 0.01 M $CaCl_2$ added. Pressure drop through the vortex diode = 3.5 bar.

3.4. Polymer Solution Viscoelasticity

Changes in viscoelasticity were observed as a result of the presence of electrolytes and the application of HC. Table 2 presents the results for the loss and storage modulus ratio under the initial condition and after 500 passes through the HC device. The effects of electrolytes differed markedly between Ca^{2+} and K^+. While Ca^{2+} slightly increased the elasticity of the initial solution, K^+ decreased it, although both ions reduced the average viscosity. This suggests that the reported thinning effect [26] may not be the only mechanism involved and may depend on the salt species. Within the linear viscoelastic zone, the studied concentrations of Ca^{2+} and K^+ exhibited opposite effects: Ca^{2+} enhanced rigidity and structural stability, whereas K^+ reduced both. Thus, Ca^{2+} appears to exert a "cementing

effect", while K^+ promotes dispersion. This behavior can be explained by the ability of Ca^{2+} to cross-link polyacrylamide chains [12,32].

Table 2. Loss modulus G″ to storage modulus G′ ratio for the different compositions and operating conditions.

Condition	Composition	Head Loss	G″/G′
Initial	1 g/L PAM	-	0.57 ± 0.07
Initial	1 g/L PAM + 0.01 M $CaCl_2$	-	0.19 ± 0.04
Initial	1 g/L PAM + 0.01 M KCl	-	6.56 ± 1.58
500 passes	1 g/L PAM	2	18,023 ± 3250
500 passes	1 g/L PAM	2.8	>20,000
500 passes	1 g/L PAM	3.5	>20,000
500 passes	1 g/L PAM + 0.01 M $CaCl_2$	3.5	>20,000
500 passes	1 g/L PAM + 0.01 M KCl	3.5	>20,000

Nonetheless, the effects of HC largely overshadowed the differences caused by salt addition. Significant reductions in elasticity were observed in all cases, with some values exceeding the instrument's detection limits. The increase in the G″/G′ ratio for treated PAM solutions without salt addition depended only marginally on the applied pressure drop. This shift reflects a tendency toward purely viscous behavior. Meanwhile, no significant differences were found between PAM solutions with and without added KCl or $CaCl_2$ after HC treatment. HC effectively eliminated all elastic properties, transforming the PAM solution into an almost purely viscous fluid. This transformation cannot be attributed solely to the presence of dissolved salts, particularly because, at the tested concentrations, the gel-like structure of the polymer remains comparable to that in distilled water [26], with only the charge screening effect being present. The changes are likely due to a generalized weakening of polymer chain-to-chain interaction forces.

4. Conclusions

HC effectively reduced the viscosity and viscoelasticity of PAM solutions, with the extent of modification strongly influenced by the number of passes. A critical molecular size limit is suggested, below which further depolymerization becomes minimal. This limitation appears to result from an intermediate size range of polymer chains that are too small to undergo mechanical shear-induced cleavage but too large to enter cavitation bubbles and be degraded by chemical mechanisms.

Salt addition was found to enhance the degradation of PAM significantly. This effect was attributed to a combination of charge screening and salting-out phenomena, which reduce intermolecular interactions, decrease hydrodynamic radius, and increase the solubility and mobility of polymer chains in the supercritical water domains attained within the cavity bubbles before implosion.

HC eliminated the elastic behavior of PAM solutions, transforming them into nearly purely viscous fluids. This transformation is likely related to a decrease in the average molecular weight. The observed plateau in the consistency index supports the idea that the HC treatment narrows the molecular weight distribution, not just causing uniform chain cleavage.

In summary, HC is a powerful tool for tailoring the rheological properties of PAM solutions. However, intrinsic limitations related to chain size and cavitation dynamics must be considered. Future optimization of HC device design may allow for further improvements in depolymerization performance.

Author Contributions: Conceptualization, methodology, investigation, software, validation, data curation, formal analysis, and writing—original draft preparation: S.N.F. and M.d.P.B.; investigation, resources, data curation, writing—review and editing, visualization, supervision, project administration, and funding acquisition: M.A.A. and M.C. All authors have read and agreed to the published version of the manuscript.

Funding: This research was funded by Universidad de Buenos Aires, grant number UBACyT 20020220100154BA.

Data Availability Statement: The original contributions presented in this study are mainly included in the article. Further inquiries can be directed to the corresponding author. The raw data supporting the conclusions of this article will be made available by the authors upon request.

Conflicts of Interest: The authors declare no conflicts of interest. The funders had no role in the design of this study; in the collection, analyses, or interpretation of data; in the writing of the manuscript; or in the decision to publish the results.

References

1. Zupanc, A.; Petkovšek, M.; Zdovc, B.; Žagar, E.; Zupanc, M. Degradation of hydroxypropyl methylcellulose (HPMC) by acoustic and hydrodynamic cavitation. *Ultrason. Sonochemistry* **2024**, *109*, 107020. [CrossRef]
2. Wang, X.; Jin, A.; Zhu, M.; Feng, C.; He, H.; Huang, Z.; Li, K.; Wang, L. Study on low-temperature plasma γ-Al_2O_3 catalytic viscosity reduction of polyacrylamide solution. *Environ. Sci. Pollut. Res.* **2023**, *30*, 36098–36111. [CrossRef] [PubMed]
3. Lim, K.Y.; Foo, K.Y. Innovation in Depolymerization Techniques. In *Depolymerization: Concepts, Progress, and Challenges Volume 2: Advances and Breakthroughs*; ACS Symposium Series; American Chemical Society: Washington, DC, USA, 2025; Chapter 2; pp. 17–40. [CrossRef]
4. Gągol, M.; Przyjazny, A.; Boczkaj, G. Wastewater treatment by means of advanced oxidation processes based on cavitation–A review. *Chem. Eng. J.* **2018**, *338*, 599–627. [CrossRef]
5. Galloni, M.G.; Fabbrizio, V.; Giannantonio, R.; Falletta, E.; Bianchi, C.L. Applications and applicability of the cavitation technology. *Curr. Opin. Chem. Eng.* **2025**, *48*, 101129. [CrossRef]
6. Kawadkar, A.S.; Gogate, P.R. Intensified depolymerization using ultrasound—A review of mechanisms, reactors, operating conditions and applications. *Chem. Eng. Process.-Process Intensif.* **2023**, *191*, 109446. [CrossRef]
7. Fleite, S.N.; Ayude, M.A.; Ranade, V.V.; Cassanello, M.C. Hydrodynamic cavitation effects on advanced oxidation processes and mass transfer: A conceptual model. *Chem. Eng. J. Adv.* **2024**, *18*, 100603. [CrossRef]
8. Pavlenko, A. Numerical Modeling of the Behavior of Bubble Clusters in Cavitation Processes. *Energies* **2024**, *17*, 1741. [CrossRef]
9. Yan, J.; Ai, S.; Yang, F.; Zhang, K.; Huang, Y. Study on mechanism of chitosan degradation with hydrodynamic cavitation. *Ultrason. Sonochemistry* **2020**, *64*, 105046. [CrossRef]
10. Prajapat, A.L.; Gogate, P.R. Depolymerization of carboxymethyl cellulose using hydrodynamic cavitation combined with ultraviolet irradiation and potassium persulfate. *Ultrason. Sonochemistry* **2019**, *51*, 258–263. [CrossRef]
11. Yin, J.-Y.; Ma, L.-Y.; Siu, K.-C.; Wu, J.-Y. Effects of Ultrasonication on the Conformational, Microstructural, and Antioxidant Properties of Konjac Glucomannan. *Appl. Sci.* **2019**, *9*, 461. [CrossRef]
12. Spildo, K.; Sæ, E.I.Ø. Effect of Charge Distribution on the Viscosity and Viscoelastic Properties of Partially Hydrolyzed Polyacrylamide. *Energy Fuels* **2015**, *29*, 5609–5617. [CrossRef]
13. Prajapat, A.L.; Gogate, P.R. Intensified depolymerization of aqueous polyacrylamide solution using combined processes based on hydrodynamic cavitation, ozone, ultraviolet light and hydrogen peroxide. *Ultrason. Sonochemistry* **2016**, *31*, 371–382. [CrossRef] [PubMed]
14. Zhang, X.; Fan, Z.; Cai, L.; Fu, Y.; Liu, J.; Liu, Q.; Tong, Q.; Qiao, S.; Sun, A. Polyacrylamide structural instability and degradation induced by nanobubbles: A molecular simulation study. *Phys. Fluids* **2025**, *37*, 022024. [CrossRef]
15. Wang, B.; Su, H.; Zhang, B. Hydrodynamic cavitation as a promising route for wastewater treatment—A review. *Chem. Eng. J.* **2021**, *412*, 128685. [CrossRef]
16. Ranade, V.V.; Bhandari, V.M.; Nagarajan, S.; Sarvothaman, V.P.; Simpson, A.T. *Hydrodynamic Cavitation a Systematic Introduction to Critical Technologies and Applications of Hydrodynamic Cavitation*; John Wiley & Sons: Hoboken, NJ, USA, 2022.
17. Simpson, A.; Ranade, V.V. 110th Anniversary: Comparison of Cavitation Devices Based on Linear and Swirling Flows: Hydrodynamic Characteristics. *Ind. Eng. Chem. Res.* **2019**, *58*, 14488–14509. [CrossRef]
18. Simpson, A.; Ranade, V.V. Flow characteristics of vortex based cavitation devices: Computational investigation on influence of operating parameters and scale. *AIChE J.* **2019**, *65*, e16675. [CrossRef]

19. Ranade, V.V.; Kulkarni, A.A.; Bhandari, V.M. Vortex Diodes as Effluent Treatment Devices. U.S. Patent No. 9,422,952B2, 23 August 2016. Available online: https://patentimages.storage.googleapis.com/7f/ae/c2/b1a4a224890f81/US9422952.pdf (accessed on 18 June 2025).
20. Ranade, N.V.; Sarvothaman, V.; Ranade, V.V. Acoustic Analysis of Vortex-based Cavitation Devices: Inception and extent of cavitation. *Ind. Eng. Chem. Res.* **2021**, *60*, 8255–8268. [CrossRef]
21. Gode, A.; Madane, K.; Ranade, V.V. Design of vortex-based cavitation devices/reactors: Influence of aspect ratio, number of inlets and shape. *Ultrason. Sonochemistry* **2023**, *101*, 106695. [CrossRef]
22. Pandit, A.V.; Sarvothaman, V.P.; Ranade, V.V. Estimation of chemical and physical effects of cavitation by analysis of cavitating single bubble dynamics. *Ultrason. Sonochemistry* **2021**, *77*, 105677. [CrossRef]
23. Thaker, A.H.; Madane, K.R.; Ranade, V.V. Influence of viscosity and device scale on pressure drop and cavitation inception: Vortex based cavitation devices. *Chem. Eng. J.* **2023**, *474*, 145943. [CrossRef]
24. Whorlow, R.W. *Rheological Techniques*, 2nd ed.; Ellis Horwood Series in Physics and Its Applications; Ellis Horwood Ltd.: Hertfordshire, UK, 1992.
25. Laun, M.; Auhl, D.; Brummer, R.; Dijkstra, D.J.; Gabriel, C.; Mangnus, M.A.; Rüllmann, M.; Zoetelief, W.; Handge, U.A. Guidelines for checking performance and verifying accuracy of rotational rheometers: Viscosity measurements in steady and oscillatory shear (IUPAC Technical Report). *Pure Appl. Chem.* **2014**, *86*, 1945–1968. [CrossRef]
26. Árok, Z.V.; Sáringer, S.; Takács, D.; Bretz, C.; Juhász, Á.; Szilagyi, I. Effect of salinity on solution properties of a partially hydrolyzed polyacrylamide. *J. Mol. Liq.* **2023**, *384*, 122192. [CrossRef]
27. Hu, J.; Fu, M.; Li, M.; Luo, Y.; Ni, S.; Hou, L. Main Controlling Factors Affecting the Viscosity of Polymer Solution due to the Influence of Polymerized Cations in High-Salt Oilfield Wastewater. *Processes* **2024**, *12*, 791. [CrossRef]
28. Sarvothaman, V.P.; Simpson, A.T.; Ranade, V.V. Modelling of vortex based hydrodynamic cavitation reactors. *Chem. Eng. J.* **2019**, *377*, 119639. [CrossRef]
29. Fleite, S.N.; Torres, R.; Lagorio, M.G.; Ranade, V.V.; Cassanello, M.C. Hydrodynamic cavitation effects over complex organic mixtures. *Chem. Eng. Res. Des.* **2024**, *204*, 371–381. [CrossRef]
30. Xu, X.; Zhang, P.; Luo, X. Synergistic mechanism of polymer and asphaltene in supercritical water oxidation treatment of polymer-containing oily sludge: Degradation pathway and nitrogen transfer. *J. Hazard. Mater.* **2025**, *494*, 138627. [CrossRef] [PubMed]
31. Davlyud, D.N.; Vorobeva, E.V.; Laevskaya, E.V.; Cherednichenko, D.V.; Vorobev, P.D. Flocculating and hydrodynamic properties of aqueous-salt solutions of acrylamide polymers. *Russ. J. Appl. Chem.* **2019**, *92*, 1135–1142. [CrossRef]
32. Bessaies-Bey, H.; Baumann, R.; Schmitz, M.; Radler, M.; Roussel, N. Effect of polyacrylamide on rheology of fresh cement pastes. *Cem. Concr. Res.* **2015**, *76*, 98–106. [CrossRef]

Disclaimer/Publisher's Note: The statements, opinions and data contained in all publications are solely those of the individual author(s) and contributor(s) and not of MDPI and/or the editor(s). MDPI and/or the editor(s) disclaim responsibility for any injury to people or property resulting from any ideas, methods, instructions or products referred to in the content.